

*На підставі теоретичних і практичних досліджень методами обчислювальної гідродинаміки розрахована геометрія фізичної моделі підрулюючого пристрою із двома ступенями свободи і зазначені необхідні фізичні умови її реалізації. Систематизовано та зведено у таблицю перелік параметрів (чинників) відповідно до експлуатаційного режиму судна, які необхідні для рішення основних рівнянь при формалізації фізичних моделей підрулюючих пристроїв*

*Ключові слова: судновий підрулюючий пристрій, деградаційний ефект, формалізація фізичної моделі, обчислювальна гідродинаміка*

*На основании теоретических и практических исследований методами вычислительной гидродинамики рассчитана геометрия физической модели подруливающего устройства с двумя степенями свободы и указаны необходимые физические условия ее реализации. Систематизирован и сведен в таблицу перечень параметров (факторов) в соответствии с эксплуатационным режимом судна, который необходим для решения основных уравнений при формализации физических моделей подруливающих устройств*

*Ключевые слова: судовой подруливающее устройство, деградационный эффект, формализация физической модели, вычислительная гидродинамика*

UDC 629.56:064.5+620.9+629.5

DOI: 10.15587/1729-4061.2017.101298

# FORMALIZATION OF DESIGN FOR PHYSICAL MODEL OF THE AZIMUTH THRUSTER WITH TWO DEGREES OF FREEDOM BY COMPUTATIONAL FLUID DYNAMICS METHODS

V. Budashko

PhD, Associate Professor

Department of technical fleet operation

National University «Odessa Maritime Academy»

Didrikhson str., 8, Odessa, Ukraine, 65029

E-mail: bvv@te.net.ua

## 1. Introduction

The development of coastal shelf of the world's ocean, from the point of view of extraction of natural resources, the use of wind energy and current, has been going on at the very high rate. Carrying out drilling operations is one of the most important components of these processes.

In contrast to drilling on land, functional drilling schemes of marine wells [1] are complicated by the behavior of water between the wellhead and the drilling unit. Among the variety of technological processes employed in these operations, commonly used are, in particular, the self-lifting (SLDR) and the semi-submersible self-propelled drilling rigs (SSDR), as well as drilling ships (Fig. 1). The main factor that influences the choice of the type of floating drilling facilities is the depth of sea at the location of drilling.

The drilling ships, due to better maneuverability and motion speed, better autonomy in comparison with SSDR [2], are used when drilling the prospecting and exploration wells in remote areas at the depths of water areas up to 3000 m. As opposed to SSDR, the drilling ships have considerable constraints for their operations depending on the sea state. Thus, during drilling, vertical pitching of the drilling ships must not exceed 3.6 m, while for SSDR – up to 5 m. The shortcomings of the latter include the low speed of motion.

The azimuthal thruster with the propeller-steering column was developed and implemented (APSC) in 1950. Over the subsequent period, these installations have gained positive reputation on the ships, which require high maneuverability under conditions of limited space. In 1990, the firm ABB Group (Sweden) put the high-torque electric motor

inside the shell of APSC gondola and installed it on the tug Seilin (Finland), having registered it under the brand name Azipod®. Since then, this type of installations has been widely used on other types of ships. At present, APSC of power up to 20 MW is the remarkable propulsive solution for the wide range of ships [3].

Recently, given the development of technology and more strict requirements for the precision of DP mode of ships, as well as to simplify maneuvers under conditions of limited operation space, ships are more and more often equipped with APSC, which can be installed both as an optional and as the main propulsion units [4]. The main task is to ensure the stability of the ship and manageability in the wide range of these types of ships.

However, during the APSC operation, the situations occur when their safe and efficient work deteriorates [5]. Thus, one variant is the case of slow motion on course by ships that lay the cables and fixing the position for SSDR and other types of ships. In order to maintain the object in the position, APSC directs the water flow under the bottom of the ship and in this case there is the probability of occurrence of the Coanda effect when the flow “sticks” to the bottom of the ship [6]. In this case, the force acting on the propeller leads to the deviation of the rowing shaft, which entails an increased wear of deadweight, propulsive and supporting bearings. Due to the design feature that locates the APSC below the waterline under the bottom of the ship, the access to diagnosis, routine maintenance and repair is hampered. The work of drilling ships is based on the dynamic positioning mode and premature failure of one of the APSCs may lead to tragic consequences, multi-billion dollar losses and technogenic disaster [7].

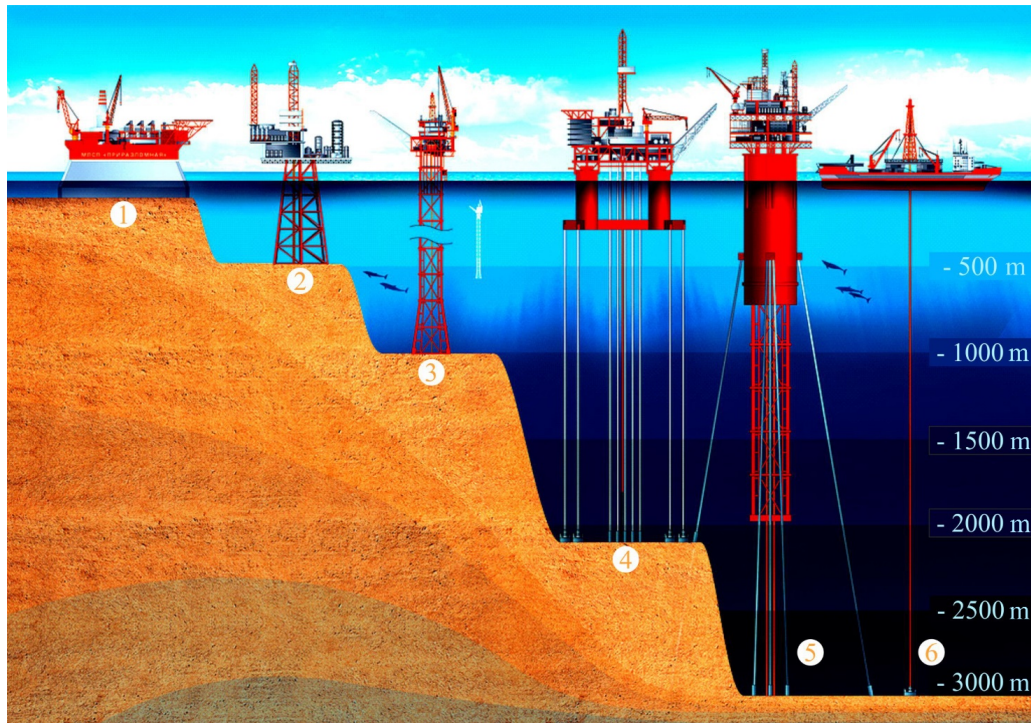


Fig. 1. Types of marine drilling means: 1, 2 – stationary drilling platforms; 3 – stationary self-lifting tower (SLDR) or the flexible tower; 4 – semi-submersible self-propelled drilling rig (SSDR) of the type TLP (tension-leg platform); 5 – platforms of the type SPAR (Single Point mooring And Reservoir); 6 – drilling ship

Unfortunately, predicting and calculating the process with detailed outline of all parameters is not possible because the occurrence of the Coanda effect is influenced by many factors, such as:

- the ship velocity, the speed and direction of propellers rotation;
- condition of the environment, chemical composition and the depth of water surface;
- the speed and direction of water flows from other APSCs that work together and are included in the system of dynamic positioning.

These factors do not make it possible to accurately predict the time of occurrence of this effect.

Depending on the technique of transferring the power to the propeller and its required need, APSC are divided into nine basic types (Fig. 2, *a–i*).

Standard modules Z-Drive made by Rolls-Royce company with input power from 250÷3700 kW (Fig. 2, *a*) to install on the tows, starting from 11 to more than 120 tonnes. Modular design allows changing the configuration, size and type of installation, in order to better satisfy the requirements of the user. These designs are available with reverse rotation of propellers to ensure high efficiency of engine with small subsidence, or with fixed pitch/controllable pitch (FPP/CPP) propellers, open or duct, with diameter matching the displacement.

APSC of the type Azippul (depending on the type of the ships) are characterized by low resistance and high efficiency that combines the advantages of thrust of the propeller with the flexibility of using the drive of capacity from 900÷5000 kW (Fig. 2, *b*). Such SP are designed for velocities of up to 24 knots while maintaining excellent maneuverability, hydrodynamic and fuel efficiency, low level of noise and vibration. Large area of rudder provides excellent course

stability; in terms of minimizing the degradation effects, the units also enable the optimization of the stern part of the hull for minimum resistance and simplified design.

APSC Contaz® (Fig. 2, *c*) with the reverse rotation of propellers provides high efficiency of the engine and reduce vibration of ships with small subsidence. Efficiency can be improved in the range of 10÷15 percent compared to conventional azimuthal thrusters. The stern FPP return the part of energy losses in the flow, as well as significant losses in rotation, which is why they are promising in terms of reducing the lower limit of power. APSC Contaz® have the wide range of the length of the stem and are ideal for passenger/car ferries and ships that operate in areas with limited terms of operating modes.

Reliable ultra-strong standard modules L-Drive (Fig. 2, *d*) are APSC designed specifically for long and reliable operation under DP modes for drilling ships and offshore drilling rigs. Compact design allows for easier installation and maintenance. There are two ways to connect the lifting actuators: flange from the middle of the ship to SP or external at the engine flange. SSC are controlled by the tools of hydraulic type.

Retractable structures of APSC models of the type UL ensure the rapid hydraulic lifting and lowering of the unit (Fig. 2, *e*) that allows reducing resistance to the motion of the ship. The UL models are designed for the horizontal drive with automatic system of disconnecting the shaft. The ULE models are designed for the vertical drive. Both are available with FPP or CPP.

APSC of the type Swing-UP (Fig. 2, *f*) in submersed position act as azimuthal engines with thrust vectoring in any required direction to propel the ship or maintenance the position. In an elevated position, with special structures located in the hull, it can function as the tunnel motor (TH of tunnel type).

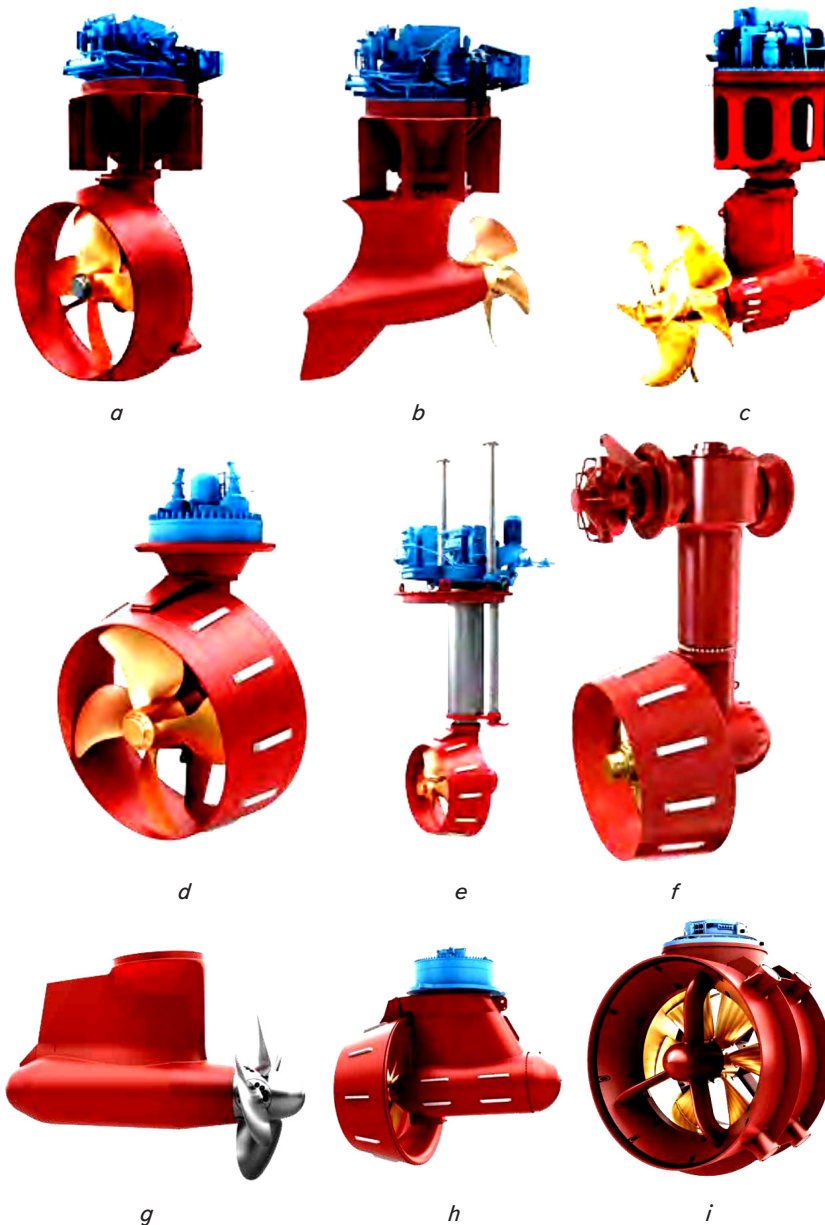


Fig. 2. Basic types of APSC: *a* – standard modules Z-Drive with power of 250÷3700 kW; *b* – modules Azippul with power of 900÷5000 kW; *c* – modules Contaz@ with power of 2200÷3700 kW; *d* – standard modules L-Drive with power of 3000÷6,500 kW; *e* – models UL/ULE with power of 580÷3800 kW; *f* – model of the type Swing-UP with power of 736÷2000 kW; *g* – model of the type ICE/HICE of ice class with power of 4000÷18,000 kW; *h* – model of the type PUSH with power of 4000÷12000 kW for ships operating on small speeds; *i* – model of the type TT-PM with power of 1000 and 1600 kW

APSC Rolls-Royce of the type Mermaid™ (Fig. 2, *g, e*) provides flexibility in the design of the ship and layout of equipment. Such designs combine the functions of propulsion engine, main propeller, steering unit and the stern thruster in one block. Ice-strengthened structures of the type ICE/HICE are specifically designed for all variants of equipment of SPP of CPC. These ships can operate under the most severe arctic conditions with the range of power from 4000 to 18000 kW (Fig. 2, *g*).

The models of the type PUSH (Fig. 2, *h*) with power from 4000 to 12000 kW are intended for operation at lower speeds, high loads and strict requirements to the con-

trol quality under an assigned operating mode. Equipped with hydrodynamically optimized nozzles to achieve maximum efficiency, such models of thrusters (THR) enable the operators to make the most of all the benefits of energy saving.

THR based on APSC of the type TT-PM (Fig. 2, *i*) is the latest design of THR by Rolls-Royce. The design uses AC electric motors with permanent magnets with power of 1000 and 1600 kW, designed for the DP modes.

Sensitivity of ships power plants (SPP) of combined propulsive complexes (CPC) to various losses depends on the types of propellers and engines, the use of various stabilizers in the design of the ship hull and the principles of change in control algorithms.

Thus, we can state that the principles of formalization in the design of physical models of THR of CPC SPP are the relevant issue. This is especially true for the process of selection and improvement of different designs of CPC and the adjustment of chosen regulators.

## 2. Literature review and problem statement

All propulsion engines can operate under modes of regulating the moment (thrust) or rotation speed but each type of the steering propeller (SP) has its own special features. Some important parameters will have slightly different values for different types of SP. Fig. 3, *a–c* shows the schematic overview of action of thrusts of various types of engines of SP.

The losses of propellers, caused by the axial influx of water, depend on the following effects that will contribute to the reduction of thrust of the propeller and the torque:

- arrival of water perpendicular to the axis of the propeller caused by the current from the ship speed or flows from other engines with the force in the direction of flow through the deviation of propeller flow. It is often referred to as the cross-combination of thrusts [8];
- the presence of cavitation for heavy loads on propellers (intake of air) leads to the decrease in pressure on the propeller blades and can occur at low immersion of the propeller due to the motion of ship across the waves [9];
- extreme conditions with large amplitudes of the motion of the ship perpendicular to the surface of water leads to the sudden drop in thrust and torque with the hysteresis effect [10];
- simultaneous reduction of thrust and reverse thrust can occur due to the interaction between the flow from SP and the hull, caused by the effects of pressure, when the small thrust of SP passes along the hull. This is referred to as the Coanda effect [11–13];

– loss of thrust of SP can be caused by the influence of the rowing flow from one engine on the neighboring engines, and lead to the significant decrease in thrust, if appropriate precautions are not taken in the algorithm of distribution of thrusts on SP [14].

The main losses when main propulsion motor (MPM) CPC SPP operate under the influence of non-determined loads is the interaction of flows of propellers (thruster-thruster interaction) and the interaction of flows with the hull (thruster-hull interaction). These effects have gained the general name in studies – degradation effects on the lines of propellers flows.

In order to evaluate and examine such phenomena, along with experimental data, the results of computation by the methods of computational fluid dynamics (CFD) are employed.

The research base in the field of calculating the hydrodynamic processes on the propellers lines of MPM of SP of CPC SPP is the Navier-Stokes equations:

$$\frac{\partial \vec{v}}{\partial t} = -(\vec{v} \nabla) \vec{v} + v_w \nabla \vec{v} - \frac{1}{\rho} \nabla P_v + \vec{f}_m, \quad \nabla \cdot \vec{v} = 0, \quad (1)$$

where  $\nabla$  is the nabla operator;  $\Delta$  is the Laplace vector operator;  $t$  is the time [s];  $v_w$  is the coefficient of kinematic viscosity,  $\times 10^{-6}$  [m<sup>2</sup>/s];  $\rho$  is the medium density [kg/m<sup>3</sup>];  $P_v$  is the flow pressure, [Pa];  $\vec{v} = (v^1, \dots, v^n)$  is the vector velocity field;  $\vec{f}_m$  is the vector field of mass forces.

For the turbulent flows of water from the propellers of MPM of SP of CPC SPP it is based on the generalized equation of Navier-Stokes (1), which holds for both laminar and turbulent fluid flow mode. However, using the given equation for the turbulent motion regime is almost impossible. In it, the input instantaneous values of velocity and pressure of the flow are the pulsating magnitudes, which is why for the turbulent regime, the task is to find the time-averaged velocities and pressures. For this purpose, they apply the Reynolds equations received based on the Navier-Stokes equation, whose all terms undergo the operation of averaging over time [15].

To obtain adequate results of dependence at the levels of flows from the propellers, the operations of averaging must take place. These operations are based on the assumption that the averaging performed on it for any turbulent flow yield the magnitude of invariables during repeated averaging [16].

Pulsating variable components are characterized by frequency and amplitude, while the mean amplitudes of pulsation are characterized by appropriate coefficients of pulsations [17]. For example, for the Reynolds-averaged Navier-Stokes (RANS) equation, the method of averaging is to replace the flow characteristics (velocity, pressure, density) with totals of the averaged and pulsating components that randomly change. In the case of stationary flow of an incompressible Newtonian fluid, the Reynolds equation are written in the form:

$$\rho \frac{\partial \bar{u}_j \bar{u}_i}{\partial x_j} = \rho \bar{f}_{mi} + \frac{\partial}{\partial x_j} \left[ -\bar{P}_v \delta_{ij} + \mu_R \left( \frac{\partial \bar{u}_i}{\partial x_j} + \frac{\partial \bar{u}_j}{\partial x_i} \right) - \rho \bar{u}'_i \bar{u}'_j \right]. \quad (2)$$

Variables averaged over time are marked in this equation with the line atop; the pulsation components – with an apostrophe. The left side of the equation (non-stationary term) describes the change in the volume of water flow motion from the propeller, due to the change over time in the averaged component of its velocity. This change is compensated for by the averaged external forces of perturbation  $\rho \bar{f}_{mi}$ , averaged by pressure forces  $\bar{P}_v \delta_{ij}$  and viscosity forces:

$$\mu_R \left( \frac{\partial \bar{u}_i}{\partial x_j} + \frac{\partial \bar{u}_j}{\partial x_i} \right),$$

where  $\mu_R$  is the medium viscosity coefficient or the coefficient of viscous friction.

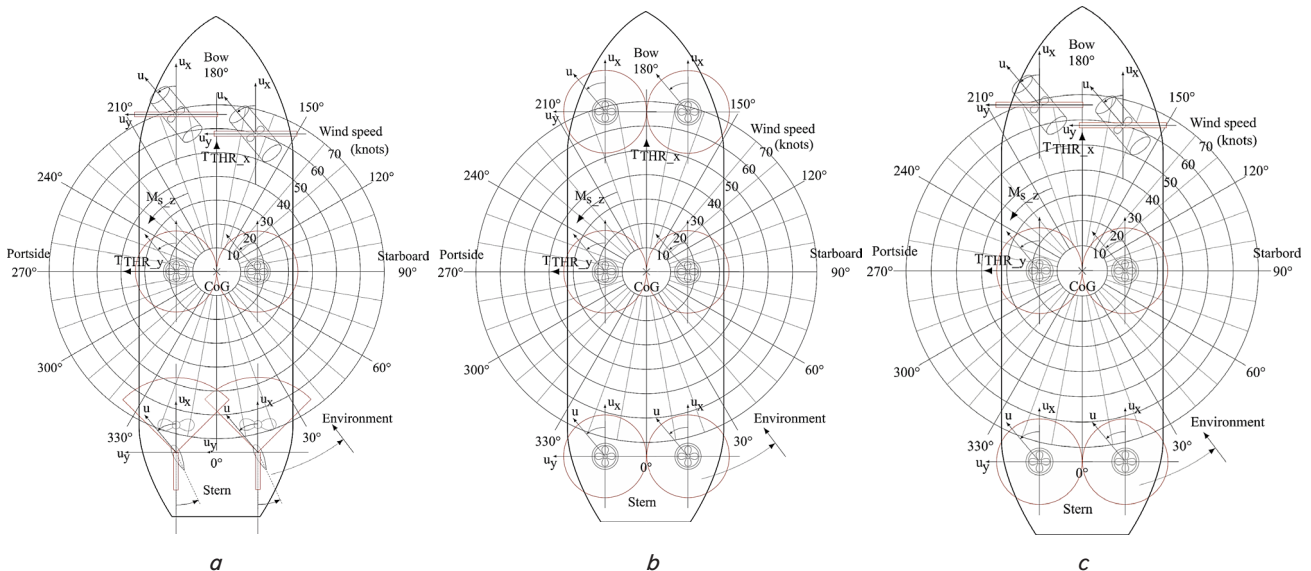


Fig. 3. Action zones of thrusts of SP on different types of assembly of ship power plants of combined propulsive complexes: *a* – action zone of thrust of devices with the classical ship power plant in the stern of the ship and tunnel thrusters in the bow; CG is the center of gravity;  $T_{THR,y}$ ,  $T_{THR,x}$  are the thrusts of the SP along their respective axes;  $M_{s,z}$  is the ship's turning point; *b* – Action zones of thrusts for the ship power plant of combined propulsive complex with full assembly of thrusters of the azimuthal type; *c* – Action zone of thrusts for the ship power plant of combined propulsive complex with the partial assembly of thrusters of the tunnel and azimuthal types

Under certain operating modes, the medium viscosity coefficient defines assigning the limits to the Reynolds number. To achieve formalization of the physical model of the multifunctional combined propulsive complex, it is necessary to consider situational factors of the environment and identifying factors of operating modes.

The right side of equation (2) includes the set voltages  $\rho u'_i u'_j$ , which take into account additional losses and the redistribution of energy in the turbulent flow at the boundary with the laminar flow. The losses are caused by the emergence of the so-called degradation effects [18].

### 3. The aim and tasks of research

The aim of present research is to develop principles of applying the methods of computational fluid dynamics for the formalization of physical models of azimuthal SP in terms of tracking the degradation effects on the flow lines of propellers.

To accomplish the set aim, the following tasks are to be solved:

- at the preparatory stage, to form the geometry of the model and to formulate required physical conditions;
- discretization of the geometry and setting the initial and boundary conditions of differential equations;
- at the stage of calculation, according to the assigned algorithm, to solve basic equations in terms of fundamental physical parameters, as well as the arrangement of results of the solution;
- to represent the results of solutions in the form of graphs, tables, as well as outline/vector diagrams, related to the original geometry.

### 4. Formalization of the physical model of the azimuthal steering propeller with two degrees of freedom

The application of computational fluid dynamics in order to analyze the effects of degradation of flow from the propeller of azimuthal engine is still, to the large degree, is an unexplored area. These effects are important for the design of ships, especially for those that operate under the mode of dynamic positioning. Testing the real models is relatively expensive and in general become affordable at the later stages in the process of designing the technical tool. As an alternative, by using computational fluid dynamics of various designs of ships and engines at an early stage of design process, the effects of interaction can be explored in an economical fashion.

A physical model of SP with two degrees of freedom, the outer view of which is shown in Fig. 4, was developed taking into account the most important properties of SP, parameters of operational modes and situational factors.

Authors of article [19] used as software for computational fluid dynamics the package Marin ReFRESKO (Reliable&Fast Rans Equations (solver for) Ships, Cavitation (and) Offshore, Netherlands) which is widely employed for the visualization of flows around different objects. ReFRESKO solves the RANS equations (averaged Reynolds Navier-Stokes equations) for multiphase non-stationary incompressible flows. The system is supplemented with the models of turbulence and volumetric-fractional equations of convective diffusion for each phase. The equations are dis-

cretized employing the method of finite volumes in physical space. Implementation is surface-oriented, which makes it possible to generate grids with arbitrary number of faces or locally cleaned grids with hanging nodes.

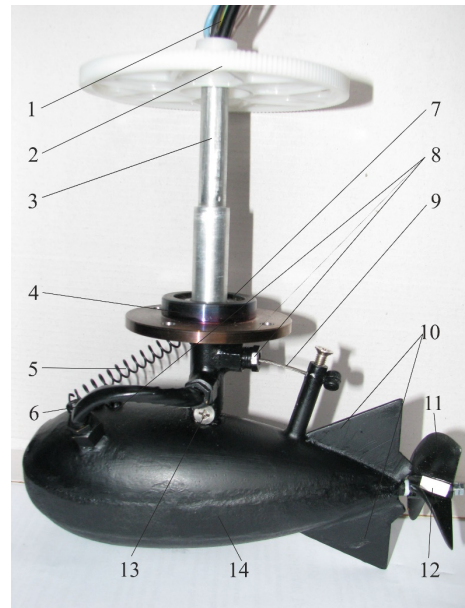


Fig. 4. Physical model of the thruster with two degrees of freedom: 1 – power cable of the propulsion asynchronous motor and the drive to change the sloping angle; 2 – anchor gear of the drive of rudderstock turning; 3 – rudderstock; 4 – bearing shield; 5 – feedback spring of the drive to change the sloping angle; 6 – power cable; 7 – supporting bearing; 8 – gland inputs; 9 – the rope of the drive to change the sloping angle; 10 – stabilization wings; 11 – screw of the fixed step; 12 – fluorescent label for the remote measurement of rotation frequency of the screw of fixed step; 13 – place of connecting the rudderstock to the body of the thruster; 14 – body of the thruster with an induction motor located inside

In order to visualize the flow of azimuthal engine of SP of CPC SPP, we accepted the model in which the propeller is represented as an Actuator Disk (AD) [20]. The model of AD replaces propeller blades by the equivalent force distribution over the entire volume of the propeller. Such model is the application of the RANS equations on the model of propeller with the possibility of obtaining the results of modeling the flow from the engine in the open water, under the hull and on the end of the hull.

According to an analysis of information about the ship, the types of propeller are applied, as well as the modifications of SP, schemes of location of medium speed diesel engine (MSDE) of SPP and their structures. The indicated schemes are the multi-bus structures with the non-uniform distribution of impedance [21]. Such uniform electrical power systems are built by the technology of Flexible Alternative Current Transmission Systems – FACTS. The application of methods of computational fluid dynamics to track the degradation effects on the flow lines of propellers is preceded by the systematization of required identification parameters and situational factors.

Calculation of effective traction efforts on propellers is the complicated condition. Iterative procedure for the solution of nonlinear equations (1), (2) is unstable for sustainable

modes as there is no priority direction of flow in the larger part of the region. That is why it is necessary to apply the approach in which the action of the flow of SP is imposed in the direction of low velocity of the motion of the ship, thus bringing the active traction effort to the assigned boundary numerical conditions. For this purpose, thrust coefficients of propellers  $K_T$  and coefficients of the torque of propellers  $K_F$  for the current velocity of the ship  $v_i$  will be defined equal to the corresponding coefficients for absolute velocity of the ship and the speed of inflow of water. The coefficients have to be formalized in accordance with the equations of similarity for the determined Reynolds and Froude numbers and coefficient of the favorable flow  $w_s$ :  $v_a = (1 - w_s)v_s$ , where, as the rule,  $0 < w_s < 0.4$ :

$$F_p = \frac{v_i}{n \cdot D_p}, \quad (3)$$

where  $n$  is the rotation frequency of propeller, rev/s;  $D_p$  is the diameter of propeller, m. Relative step of propeller and its effectiveness in the open water are defined as the ratio of the actual work of propeller to obtain the force of traction to the work required to overcome the torque of thrust on the shaft. The values of Reynolds and Froude numbers for the limits of boundary conditions must be such that the flows of function and the force acting on SP are not under the influence of perturbing forces.

Fig. 5, *a-d* shows characteristics of the flows, and the components of x-velocities of SP for the model UL/ULE (Fig. 3, *e*) of power 1500 kW. The figures display significant recirculation zones near the stern stanchion that causes an increase in the load on the rotating axis (rudderstock) and external nozzle. This fact confirms the necessity of application of complex functions for calculating the energy indicators in the intersections of energy fluxes from MSDE to the engines of SP of CPC SPP.

The corresponding (3) force of propeller thrust (CPP or FPP) of SP will be calculated based on the values of two radii (radius along the edge of propeller  $R_p$  and radius of intersection of the propeller blade  $r_p$  and thickness of the propeller blade  $b_p$ ). These parameters can be unambiguously determined as the axial characteristics of blades from their intersection. Axial and tangential forces will be determined based on the thrust and torque of the propeller that is simulated. Axial forces  $F_x, F_y, F_z$  – as algebraic distribution that is scaled and integrated to the required thrust (3). The tangential force is determined by the actual value of propeller thrust  $T_d$  [22] taking into account properties of feeding voltage [23] and it is interrelated to such properties of propellers as the step ratio of propeller  $p_D$  ( $H_p/D_p$ ). That is, all preliminary calculations of torques acting on the lines of propeller shafts of SP of CPC SPP will be carried out in the way given below:

$$\frac{F_x(\hat{r}), F_y(\hat{r})}{F} = \left( \frac{a + \hat{r}}{a + 1} \right)^m \left( \frac{b + 1 - \hat{r}}{b + 1} \right)^n,$$

where

$$\hat{r} = \frac{r - r_p}{R_p - r_p}, \quad (r_p \leq r \leq R_p), \quad (4)$$

$$T_p = \int_{-\pi}^{\pi} \int_0^1 F_x(\hat{r}), F_y(\hat{r}) d\hat{r} d\theta. \quad (5)$$

Distribution of axial forces (3) is parameterized according to the values of identification coefficients  $a, b, m, n$ , or the so-called characteristic markers of energy flux (situational factors) characterize the particular operational mode. The nonzero distribution of axial component of the force can be established over the entire range ( $r_p \leq r \leq R_p$ ) by careful selection of parameters  $a$  and  $b$ . The values of integral components correspond to the selected direction of propeller thrust  $T_p$ .

In turn, tangential components of thrusts and torques are calculated as follows:

$$\frac{F_\theta}{F_x, F_y}(\hat{r}) = \frac{H_p/D_p \times R_p}{\pi \times r}, \quad (6)$$

$$M_p = \int_{-\pi}^{\pi} \int_{r_p}^{R_p} r \times F_\theta(\hat{r}) d\hat{r} d\theta. \quad (7)$$

Fig. 6, *a-d* shows the visualization of force flows from an azimuthal engine of SP of SPP CPC executed by the above technique. The flows are represented as actuator disk (AD), where it is visible (Fig. 6, *c*). One can see that along the rotating guides there occurs the capturing of output flow to the lines of the recirculation zone. This effect leads to the emergence (Fig. 6, *d*) of recirculation zones on the y-plane and identification of turbulent areas with relative coefficients of vortex viscosity  $\mu_v/\mu_w$ .

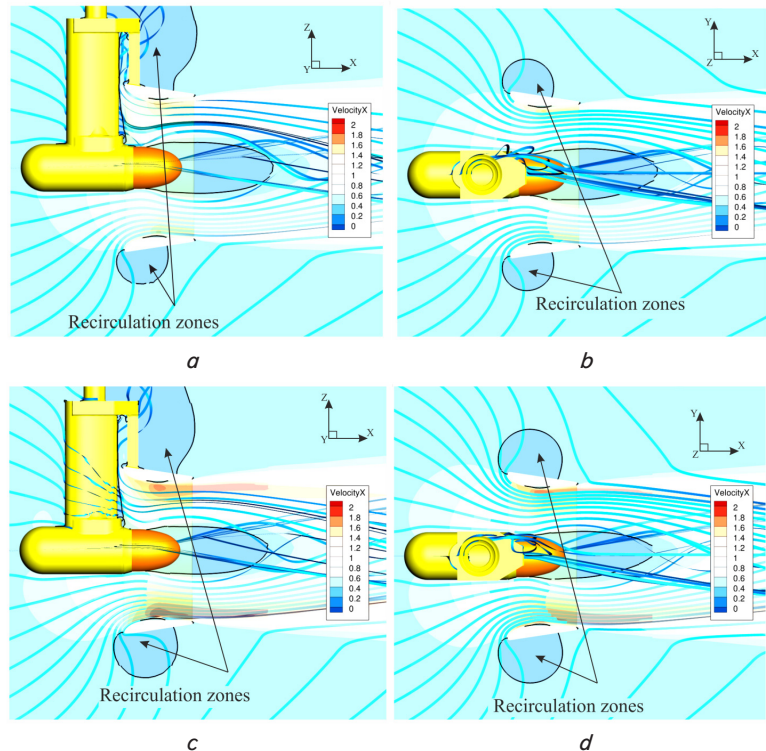


Fig. 5. Characteristics of flows and components of x-velocities of the thruster of the model UL/ULE with power of 1500 kW: *a, b* – for 70 % of the rated power on propeller shaft (side view and top view, respectively); *c, d* – for 100 % of the rated power on propeller shaft (side view and top view, respectively)

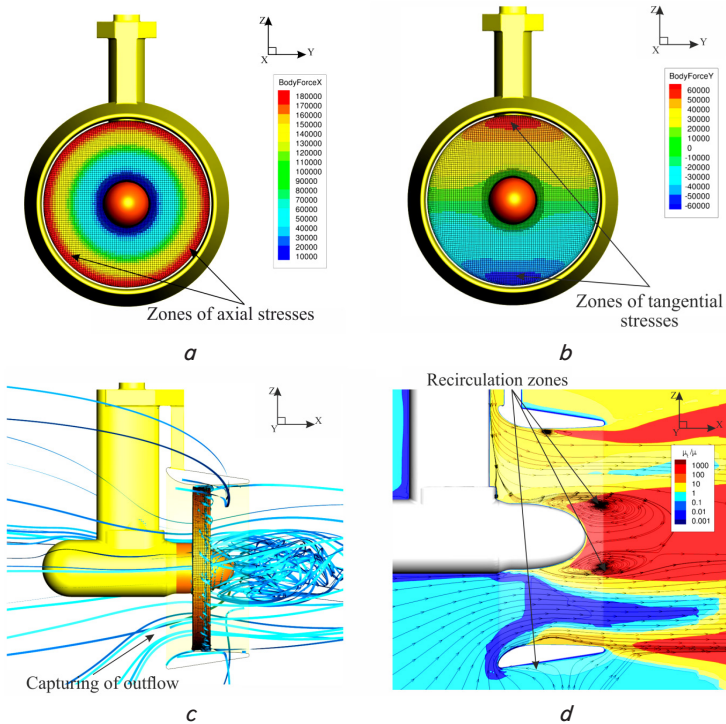


Fig. 6. Visualization of flow from azimuthal engine of SP of CPC SPP in the form of actuator disk (AD): *a* – axial and *b* – tangential components of force flows with identified zones of stress; *c* – capturing of the outflow to the lines of recirculation zone on rotating guides; *d* – recirculation zones on the *y*-plane and identifications of turbulent regions with relative coefficients of vortex viscosity  $\mu_t/\mu_w$

On the other hand, the above recirculation zones give rise to degradation effects. Fig. 7, *a–d* shows comparative analysis of trajectories of components of *x*-velocities of the propeller flow of SP. The measurements were carried out in the intersection of the flow of azimuthal propeller along the axis of rotation with dimensions in units of the propeller diameter  $D_p$ .

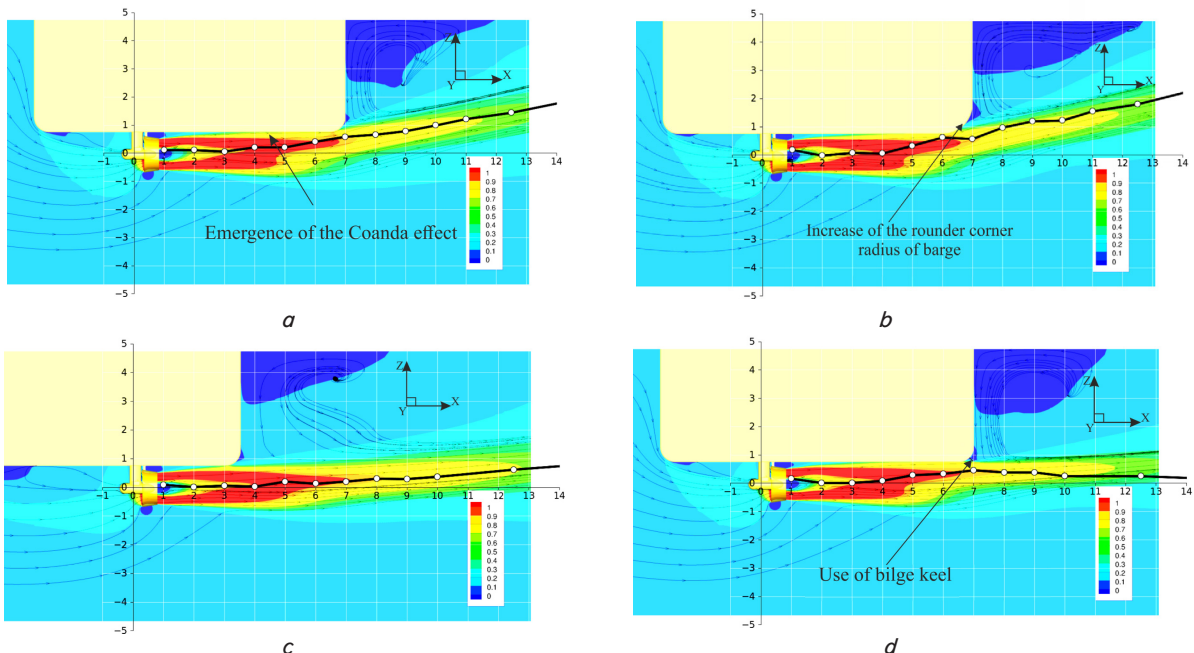


Fig. 7. Comparative analysis of trajectories of components of *x*-velocities of the propeller flow of the thruster by measurement results: emergence of the Coanda effect: *a* – standard radius of rounding the hold hull; *b* – increased radius of the rounded hold hull; *c* – reducing the sticking of flow by moving the fastening point of rudderstock of the thruster closer to the edge of the hull; *d* – use of hold keel on the envelope line of the hull

As the summary, it should be noted that notwithstanding the possibility to increase the number of intersections of measurements, some points along the trajectory remain inaccessible, which makes it impossible to fully analyze effectiveness of the proposed methods of dealing with the above mentioned effects. That is why preliminary results of formalization of the physical model of the thruster come down to determining the Reynolds and Froude numbers (3) for the zero-velocity model of the ship.

### 5. Discussion of results of calculating the power components of radial distribution of thrusts in the physical model of thruster

Fig. 8, 9 show comparative results of the two sets of parameters for power components of radial distribution of SP thrusts in the moving coordinate system. The values of the components of forces are not given on graphs because the distribution is scaled for the assigned thrust and torque.

Data were calculated for the model of SP whose identification parameters and situational factors of CPC SPP are given in Table 1. The initial selection of parameters of axial forces of the model was conducted according to equation (4), and then, taking into account the data received in [24] for the model of SP AD, these initial assumptions were refined. By analyzing results for the open water at 100 % propeller rotation velocity, we found the following set of identification parameters of the physical model of SP for maximum thrust:

$$(a, b, n, m)^* = (0; 0; 1.45; 0.06). \tag{8}$$

Table 1

Identification parameters and situational factors of CPC SPP of the model of the ship of the type Supply Ship

Parameter (factor)	Characteristic of parameter (factor) in accordance with the operating mode
$D_p$	Propeller diameter
$\lambda(H_p)$	Propeller relative step
$K_T$	Propeller thrust coefficient
$t_s$	Horizontal retention ratio
$n$	Rotation frequency
$n_N$	Rotation speed
$P_v$	Flow pressure
$H_p/D_p$	Propellers constructive step
$T_p, T_{THR}, T_d$	Propellers thrust, thrust of thruster, real value of propeller thrust
$R_p$	Propeller radius
$R_n$	Reynolds number
$M_p$	Propeller torque
$v_a$	Water inflow rate on the propeller plane
$v_s$	Ship absolute velocity
$v_i$	Current ship velocity
$F_y, F_x$	The force acting on the ship lengthwise $l_s$
$F_h, F_y$	The force acting on the ship widthwise $h_s$ that predetermines the appropriate angle of heel
$F_z$	The force acting on the ship in the direction of motion that predetermines the appropriate yaw angle
$l_s, l_M$	Length, respectively, ( $s$ ) – of the ship (to be assigned), and ( $M$ ) – of the model of the ship (to be calculated)
$b_s, b_M$	Width, respectively, ( $s$ ) – of the ship (to be assigned), and ( $M$ ) – of the model of the ship (to be calculated)
$h_s, h_M$	Subsidence, respectively, ( $s$ ) – of the ship, and ( $M$ ) – of the model of the ship
$v_{sx} (us)$	Velocity of longitudinal motion of the ship in the Cartesian coordinate system
$v_{sy} (vs)$	Velocity of lateral motion of the ship in the Cartesian coordinate system
$v_{sr} (rs)$	Velocity of yaw of the ship in the Cartesian coordinate system
$v_{saxi}$	Axial component of velocity of the motion of the ship in the cylindrical coordinate system
$v_{stg}$	Tangential component of velocity of the motion of the ship in the cylindrical coordinate system
$\mu_w$	Dynamic viscosity coefficient
$\nu_w$	Kinematic viscosity coefficient of turbulent flow
$\rho$	Water density
$\tau_T$	Vector of thrust and torque
$\omega$	Rotation frequency

Iteration solution (3)–(7) for the found parameters (8) and corresponding coefficients of similarity allows us to formalize the Reynolds and Froude numbers for zero velocity of the model of the ship:  $R_n=4.405 \times 10^6$ ;  $F_r=3.124$ . In this case, the ratio between propeller diameters of the model and an actual ship should be such as to ensure maintaining the similarity of appropriate thrusts (6) and torques (7).

Fig. 8, 9 illustrate that the proposed method allowed us to specify the components of axial and the tangential forces of radial distribution of SP thrusts within the limits of 2.7–5.1 %.

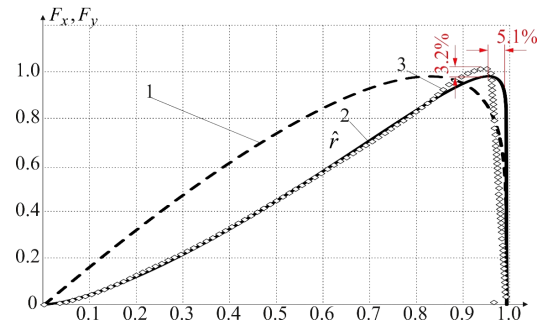


Fig. 8. Components of axial forces, proportional to the radius of the envelope line of propeller blades: 1 – initial parameters according to the boundary conditions of operating mode and situational factors (Table 1); 2 – selected parameters; 3 – according to pre-set specifications

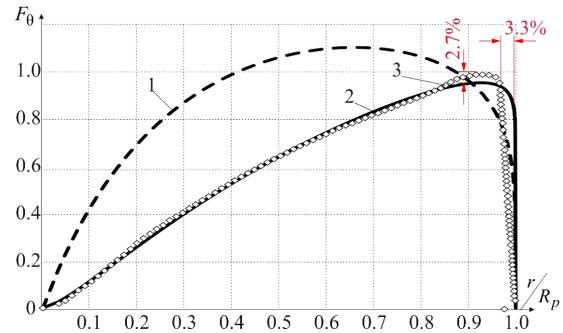


Fig. 9. Components of tangential forces, proportional to the radius of propeller: 1 – initial parameters according to the boundary conditions of operating mode and situational factors (Table 1); 2 – selected parameters; 3 – according to pre-set specifications

According to (8), the largest deviation of similarity coefficients occurs in the region of 85–100 % of the rated propeller thrust. The value of corrective factors depending on the propeller flow direction relative to the plane of motion of the ship is within the few hundredths of the percent.

When analyzing preliminary results of an analysis, we see that on the flow line from SP propeller there are significant tangential forces. There is also the “sticking” of the flow to the ship hull, which creates the degradation of thrust, reduction in the coefficient of useful action of propeller  $\eta_{pF}$  for the given value of  $K_F$  and increase in the coefficient of relative vortex viscosity  $\mu_v \mu_w$ . This leads to excessive stress on the suspended structure of SP, which creates mechanical stresses that damage the most critical design details: bearings, seals, and shaft. In addition, it worsens such operating regime of the ship as the dynamic positioning. Results of the analysis and practice of manufacturing such units reveal that the most common technique for eliminating these effects is the use of nozzles, tilted relative to the plane of the hull bottom at about 7 degrees. This solution does not avoid such effects either, and significantly reduces the efficiency of the unit, which is associated with increased consumption of fuel and pollution of the environment.

The major unexplored problem in that direction is how to impede the free fluid coming from one side of the flow. The turbulence created in the region of low pressure contributes to the emergence of significant tangential forces that act on the rudderstock of SP perpendicular to the flow direction. They do not completely solve the problem on increasing the radius of rounding the hold hull (Fig. 7, b), moving the point



of fixing the rudderstock of SP closer to the edge of the hull (Fig. 7, c) and use of hold keel on the envelope line of the hull (Fig. 7, d).

Results of the study are protected by appropriate patents on useful models [25–27], and implemented in the developed decision support system when designing and examining the CPC SPP.

---

## 6. Conclusions

---

1. We calculated the geometry of physical model of the thruster with two degrees of freedom and specified the required physical conditions for its implementation. For the zero-velocity model of the ship: Reynolds number  $R_n=4.405 \times 10^6$ ; Froude number  $F_r=3.124$ .

2. We formalized geometric parameters of the model, assigned the initial and boundary conditions of differential equations that describe behavior of flows of propellers in the

recirculation zones and coefficients, which take into account the existence of degradation effects. Components of the axial and tangential forces of the radial distribution of SP thrusts are refined within the limits of 2.7–5.1 %.

3. According to the assigned algorithm, we obtained solutions to basic equations in terms of fundamental physical parameters, as well as arranged the results of solutions. The largest deviation of similarity coefficients is in the region of 85–100 % of the rated propeller thrust.

4. We received dependences of adjustment factors that affect the components of thrusts and torques proportional to the radius of the model and the actual SP, related to the original geometry. The value of corrective factors depending on the propeller flow direction relative to the plane of motion of the ship is within the few hundredths of the percent. We systematized and compiled in the table the list of parameters (factors) according to the operating mode of the ship, which are required for solving the basic equations in the formalization of physical models of thrusters.

---

## References

1. Wang, F. Design and implementation of a triple-redundant dynamic positioning control system for deepwater drilling rigs [Text] / F. Wang, M. Lv, F. Xu // *Applied Ocean Research*. – 2016. – Vol. 57. – P. 140–151. doi: 10.1016/j.apor.2016.03.007
2. Ryu, M. Prediction and improvement of the solid particles transfer rate for the bulk handling system design of offshore drilling vessels [Text] / M. Ryu, D. S. Jeon, Y. Kim // *International Journal of Naval Architecture and Ocean Engineering*. – 2015. – Vol. 7, Issue 6. – P. 964–978. doi: 10.1515/ijnaoe-2015-0067
3. Azimuthing Electric Propulsion Drive [Text]. – Available at: [http://www04.abb.com/global/seitp/seitp202.nsf/0/589ea2a5cd61753ec12570c9002ab1d1/\\$file/AzipodNew.pdf](http://www04.abb.com/global/seitp/seitp202.nsf/0/589ea2a5cd61753ec12570c9002ab1d1/$file/AzipodNew.pdf)
4. Azipod Propulsion System [Text]. – Available at: <http://www.dieselduck.info/machine/02%20propulsion/2006%20Introduction%20to%20Azipod%20Propulsion.pdf>
5. Kobylinski, L. Problems of Handling Ships Equipped with Azipod Propulsion Systems [Text] / L. Kobylinski // *Prace naukowe politechniki warszawskiej*. – 2013. – Issue 95. – P. 232–245. – Available at: <https://pbn.nauka.gov.pl/polindex-webapp/browse/article/article-f315dfd7-df06-463e-8de7-b553f8c232db>
6. Cozijn, H. Analysis of the velocities in the wake of an azimuthing thruster, using PIV measurements and CFD calculations [Text] / H. Cozijn, R. Hallmann, A. Koop // *Dynamic positioning conference: thrusters session*. – 2010. – Available at: <http://www.refresco.org/wp-content/uploads/2015/05/2010-MTS-DP-Cozijn-Hallmann-Koop.pdf>
7. Final report on the investigation of the Macondo well blowout [Text]. – Deepwater horizon study group. – 2011. – Available at: [http://ccrm.berkeley.edu/pdfs\\_papers/bea\\_pdfs/dhsgfinalreport-march2011-tag.pdf](http://ccrm.berkeley.edu/pdfs_papers/bea_pdfs/dhsgfinalreport-march2011-tag.pdf)
8. Palmer, A. Modelling Tunnel Thrusters for Autonomous Underwater Vehicles [Text] / A. Palmer, G. E. Hearn, P. Stevenson // *IFAC Proceedings Volumes*. – 2008. – Vol. 41, Issue 1. – P. 91–96. doi: 10.3182/20080408-3-ie-4914.00017
9. Taskar, B. The effect of waves on engine-propeller dynamics and propulsion performance of ships [Text] / B. Taskar, K. K. Yum, S. Steen, E. Pedersen // *Ocean Engineering*. – 2016. – Vol. 122. – P. 262–277. doi: 10.1016/j.oceaneng.2016.06.034
10. Jian, L. Numerical investigation into effects on momentum thrust by nozzle's geometric parameters in water jet propulsion system of autonomous underwater vehicles [Text] / L. Jian, L. Xiwen, Z. Zuti, L. Xiaohui, Z. Yuquan // *Ocean Engineering*. – 2016. – Vol. 123. – P. 327–345. doi: 10.1016/j.oceaneng.2016.07.041
11. Sordalen, O. J. Optimal thrust allocation for marine vessels [Text] / O. J. Sordalen // *Control Engineering Practice*. – 1997. – Vol. 5, Issue 9. – P. 1223–1231. doi: 10.1016/s0967-0661(97)84361-4
12. Arditti, F. Experimental Analysis of a Thrust Allocation Algorithm for DP Systems Considering the Interference between Thrusters and Thruster–Hull [Text] / F. Arditti, E. A. Tannuri // *IFAC Proceedings Volumes*. – 2012. – Vol. 45, Issue 27. – P. 43–48. doi: 10.3182/20120919-3-it-2046.00008
13. Budashko, V. Physical model of degradation effect by interaction azimuthal flow with hull of ship [Text] / V. Budashko, V. Nikolskiy, O. Onishchenko, S. Khniunin // *Proceeding Book of International Conference on Engine Room Simulators (ICERS12)*. – Istanbul: Istanbul Technical University, Maritime Faculty, 2015. – P. 49–53.
14. Nikolskiy, V. The monitoring system of the Coanda effect for the tension-leg platform's [Text] / V. Nikolskiy, V. Budashko, S. Khniunin // *Proceeding Book of International Conference on Engine Room Simulators (ICERS12)*. – Istanbul: Istanbul Technical University, Maritime Faculty, 2015. – P. 45–49.
15. Mauro, F. Advantages and disadvantages of thruster allocation procedures in preliminary dynamic positioning predictions [Text] / F. Mauro, R. Nabergoj // *Ocean Engineering*. – 2016. – Vol. 123. – P. 96–102. doi: 10.1016/j.oceaneng.2016.06.045

16. Xiao, H. Quantifying and reducing model-form uncertainties in Reynolds-averaged Navier-Stokes simulations: A data-driven, physics-informed Bayesian approach [Text] / H. Xiao, J.-L. Wu, J.-X. Wang, R. Sun, C. J. Roy // *Journal of Computational Physics*. – 2016. – Vol. 324. – P. 115–136. doi: 10.1016/j.jcp.2016.07.038
17. Mishra, C. Rolling element bearing defect diagnosis under variable speed operation through angle synchronous averaging of wavelet de-noised estimate [Text] / C. Mishra, A. K. Samantaray, G. Chakraborty // *Mechanical Systems and Signal Processing*. – 2016. – Vol. 72-73. – P. 206–222. doi: 10.1016/j.ymssp.2015.10.019
18. Saha, N. Speed control with torque ripple reduction of switched reluctance motor by Hybrid Many Optimizing Liaison Gravitational Search technique [Text] / N. Saha, S. Panda // *Engineering Science and Technology, an International Journal*. – 2016. doi: 10.1016/j.jestch.2016.11.018
19. Maciel, P. Modelling Thruster-Hull Interaction with CFD [Text] / P. Maciel, A. Koop, G. Vaz // *OMAE ASME 32nd International Conference on Ocean, Offshore and Arctic Engineering*. – France, 2013. – Available at: <http://www.marin.nl/web/Publications/Publication-items/Modelling-ThrusterHull-Interaction-with-CFD.htm>
20. Thiebot, J. Modelling the effect of large arrays of tidal turbines with depth-averaged Actuator Disks [Text] / J. Thiebot, S. Guillou, V. T. Nguyen // *Ocean Engineering*. – 2016. – Vol. 126. – P. 265–275. doi: 10.1016/j.oceaneng.2016.09.021
21. Budashko, V. V. Udoskonalennja systemy upravlinnja pidruljujuchym prystrojem kombinovanogo propul'syvnogo kompleksu [Improving management system combined thruster propulsion systems] [Text] / V. V. Budashko, O. A. Onishchenko // *Bulletin of NTU "KhPI"*. – 2014. – Issue 38 (1081). – P. 45–51. – Available at: [http://repository.kpi.kharkov.ua/bitstream/KhPI-Press/13378/1/vestnik\\_HPI\\_2014\\_38\\_Budashko\\_Udoskonalennia.pdf](http://repository.kpi.kharkov.ua/bitstream/KhPI-Press/13378/1/vestnik_HPI_2014_38_Budashko_Udoskonalennia.pdf)
22. Budashko, V. V. Implementarniy podhod pri modelirovanii energeticheskikh protsessov dinamicheski pozitsioniruyushego sudna [Implementation approaches during simulation processes for a dynamically positioned ship] [Text] / V. V. Budashko // *Electrical engineering & electromechanics*. – 2015. – Issue 6. – P. 14–19.
23. Boiko, A. A. Synthesis and research of automatic balancing system of voltage converter fed induction motor currents [Text] / A. A. Boiko, V. V. Budashko, E. A. Yushkov, N. A. Boiko // *Eastern-European Journal of Enterprise Technologies*. – 2016. – Vol. 1, Issue 2 (79). – P. 22–34. doi: 10.15587/1729-4061.2016.60544
24. Budashko, V. V. Fizicheskoe modelirovanie mnogofunktsional'nogo propul'sivnogo kompleksa [Physical modeling of multi-propulsion complex] [Text] / V. V. Budashko, O. A. Onishchenko, E. A. Yushkov // *Zbirnyk naukovykh prac' Vijs'kovoï akademii' (m. Odesa). Tehnichni nauky*. – 2014. – Issue 2. – P. 88–92. – Available at: [http://zbirnyk.vaodessa.org.ua/images/zbirnyk\\_2/13.PDF](http://zbirnyk.vaodessa.org.ua/images/zbirnyk_2/13.PDF)
25. Pat. No. 100819 UA. Sudova systema monitorynhu dlya poperedzhennya efektu Koanda [Ship monitoring system for the prevention of Coanda effect] [Text] / Budashko V. V., Nikolskyi V. V., Khniunin S. H. – No. u201501854; declared: 02.03.2015; published: 10.08.2015, Bul. No. 15. – Available at: <http://base.uipv.org/searchINV/search.php?action=viewdetails&IdClaim=215069>
26. Pat. No. 108074 UA. Systema impul'sno-fazovoho upravlinnya elektropryvodom sudnovoyi hvynto-kermovoyi ustanovky [The pulse-phase control system of electric ship propeller-steering plant] [Text] / Budashko V. V., Yushkov E. A. – No. u201601510; declared: 18.02.2016; published: 24.06.2016, Bul. No. 12. – Available at: <http://base.uipv.org/searchINV/search.php?action=viewdetails&IdClaim=224863>
27. Pat. No. 107006 UA. Sudova systema monitorynhu dlya poperedzhennya efektu Koanda [Ship system for monitoring for preventing the Coanda effect] [Text] / Khnyunin S. H., Nikolskyi V. V., Budashko V. V. – No. u201512962; declared: 28.12.2015; published: 10.05.2016, Bul. No. 9. – Available at: <http://base.uipv.org/searchINV/search.php?action=viewdetails&IdClaim=223437>
28. Budashko, V. Decision support system's concept for design of combined propulsion complexes [Text] / V. Budashko, V. Nikolskyi, O. Onishchenko, S. Khniunin // *Eastern-European Journal of Enterprise Technologies*. – 2016. – Vol. 3, Issue 8 (81). – P. 10–21. doi: 10.15587/1729-4061.2016.72543